

## **A new type of magnetic pump with coupled mechanical vibration and electromagnetic force**

**Hiroyuki Yaguchi<sup>1\*</sup>, Toshiki Mishina<sup>1</sup> and Kazumi Ishikawa<sup>1</sup>**

<sup>1</sup>Faculty of Mechanical Engineering, Tohoku Gakuin University,  
1-13-1 Chuo, Tagajo, Miyagi, Japan

\*Email: [yaguchi@mail.tohoku-gakuin.ac.jp](mailto:yaguchi@mail.tohoku-gakuin.ac.jp)

Phone: +81 22368710; Fax: +81 223687070

### **ABSTRACT**

There is a demand for intravenous drips for medical sites and for liquid delivery of microfluidic chips in the field of chemical analysis. Furthermore, in these chemical analysis and medical pumps, disposable is often required. In this paper, a new pump capable of disposable having a size of 19 mm in outer diameter and 56 mm in length combining electromagnetic force and mechanical vibration was proposed. In the experiment, optimization of casing and discharge valve of this pump was examined and tested. Next, by attaching an iron plate to the iron core of the electromagnet, a method of increasing the strength of the magnetic field at one pole of the electromagnet without changing the magnetic circuit of the pump was suggested. Due to optimized design and utilization of asymmetric magnetic field, the maximum efficiency of the pump was 10.7 %. Furthermore, it was shown that this pump can deliver water to the pumping head exceeding 1000 mm.

**Keywords:** magnetic pump; vibration; pumping head; efficiency; mass flow; asymmetric magnetic field.

### **INTRODUCTION**

Pumps with high power and efficiency are highly demanded in various industrial fields and numerous researches have been conducted. Among them, for axial flow pumps [1], centrifugal pumps [2-4], mixed-flow pump [5-6], positive displacement pumps [7-8] and rotary pumps [9-12], the operating principle of these preexisting pumps is almost completely established. Improvements in the output and efficiency characteristics of these pumps depend on the built-in electromagnetic motors. By development of the electromagnetic motor with high efficiency in recent years, the centrifugal pump having the efficiency of about 90 % have been studied [13-14].

On the other hand, there is a demand for intravenous drips at medical sites and for liquid delivery of microfluidic chips in the field of chemical analysis. Furthermore, in these chemical analysis and medical pumps, disposable is often required. Based on the above considerations, many studies with regard to a new type of the pump have investigated. Previously proposed typical methods include the following: electromagnet [15-16], solenoid [17] electrostatic [18], piezoelectric [19-22], super magnetostriction [23-26], type using external magnetic field [27-29], type using elasticity of shape memory alloy [30-31], and

type using electro-hydrodynamic [32]. For the above-mentioned new type pumps, the flow rate characteristics have been elucidated in detail. However, its efficiency has not been clarified. No pumps with efficiencies exceeding 10 % are found in these studies. Furthermore, the pump having a size of about 20 mm in outer diameter and 50 mm in length and capable of disposable has not yet been developed. Considering recent high performance of permanent magnets, development of a new pump of electromagnetic-mechanical vibration type is an important problem.

In this paper, a new small size pump combining electromagnetic force and mechanical vibration was proposed. The small size pump of vibration type with an outer diameter of 19 mm and a height of 56 mm was prototyped, and the optimum design of the pump shape was carried out. This pump demonstrated a maximum efficiency of 6.0 % with a pumping head of 200 mm. By attaching an iron plate to the iron core of an electromagnet, a method of increasing the strength of the magnetic field at one pole of the electromagnet without changing the magnetic circuit was suggested. By the generation of an asymmetric magnetic field due to the addition of the iron material, the maximum efficiency of the pump was 10.7 %. In addition, this small size pump has a very simple structure and can deliver water to the pumping head exceeding 1000 mm.

### **STRUCTURE OF MAGNETIC PUMP**

Figure 1 shows a diagram of the magnetic pump prototyped for liquid delivery of various fluids. This pump is divided into a head part and a propulsion part. The head part is made of an acrylic material having an outer diameter of 19 mm, an inner diameter of 15 mm and a height of 18 mm. This head part has a discharge port with an outer diameter of 6 mm. In the propulsion part, a vibration component is inserted in an acrylic pipe having an outer diameter of 19 mm and an inner diameter of 15 mm, a height of 37 mm and a discharge valve is attached to the upper part. The propulsion part has a suction port with an outer diameter of 6 mm at a position 9 mm from the bottom. Thus, the magnetic pump consists of a permanent magnet and a translational spring constituting the vibration component, the discharge valve and the acrylic casing with a support base. The permanent magnet is cylindrical NdFeB and is magnetized in the axial direction. The permanent magnet was 12 mm in diameter and 5 mm in height. The surface magnetic flux density measured using a tesla meter was 358 mT. The translational spring was a stainless steel compression coil type having an outer diameter of 12 mm, a free length of 25 mm, and a spring constant  $k$  of 2,691 N/m.

The vibration component was constructed of the translational spring and the permanent magnet. An electromagnet was inserted in the translational spring. The electromagnet consists of an iron core having a diameter of 3.4 mm and a length of 21 mm with 1130 turns of 0.12-mm-diameter copper wire. The electrical resistance of the electromagnet is 12.4  $\Omega$ . The gap between the electromagnet and the permanent magnet in the static condition is 3 mm.

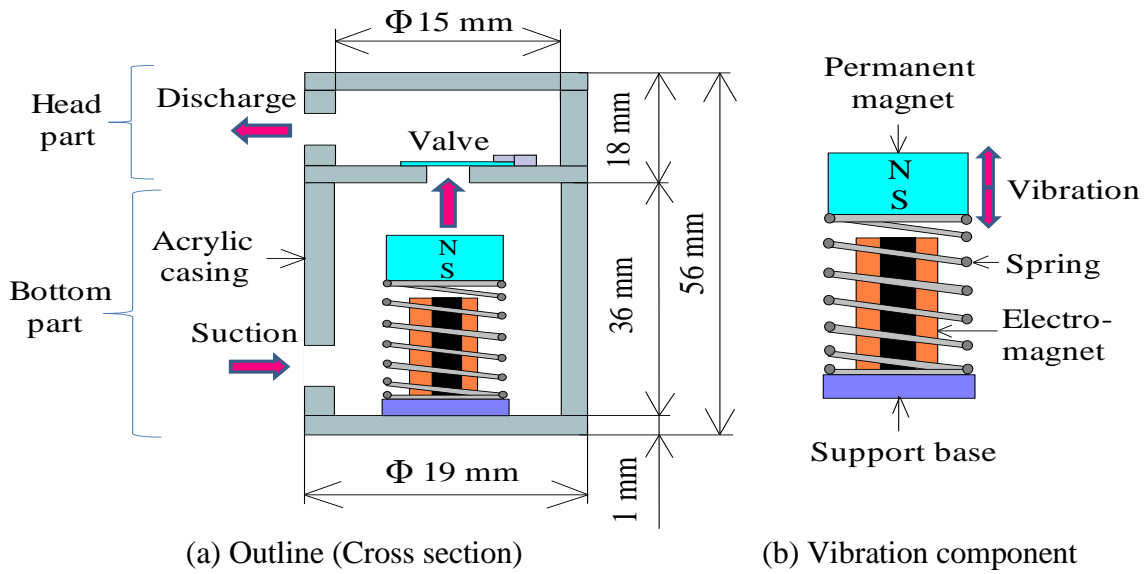


Figure 1. Structure of magnetic pump.

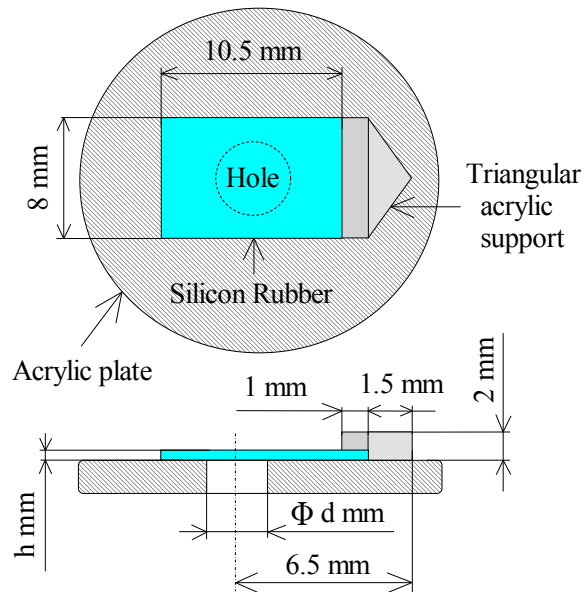


Figure 2. Detail of valve part.

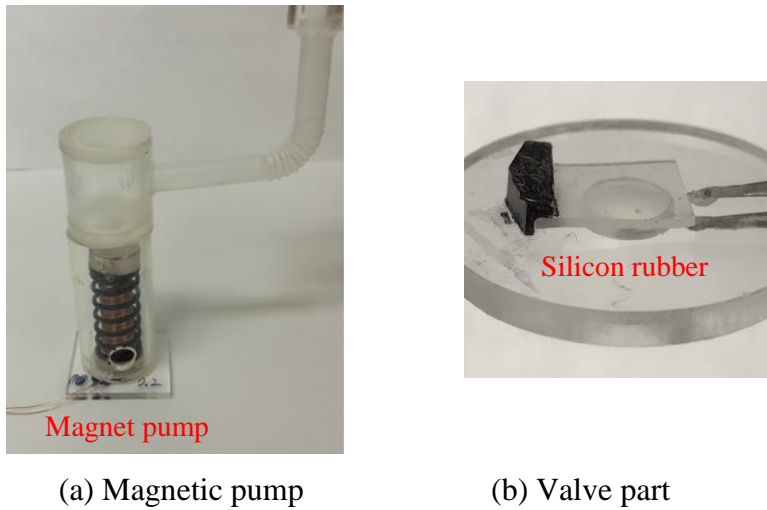


Figure 3. Photographs of magnetic pump and valve part.

The structure of the prototype valve was shown in Figure 2. A triangular acrylic support was attached to an acrylic plate having a thickness of 2 mm, an outer diameter of 19 mm, and an inner diameter of  $d$  mm. The dimension of thin silicon material is 8 mm in width, 10.5 mm in length and  $h$  mm in thickness. By attaching the thin silicon material to this triangular acrylic support, stable bending stiffness of the valve was obtained. Details of dimension in this valve are shown in Figure 2. The pump is inserted into fluid, and the vibration component vibrates by the excitation of the electromagnet. The pump has a height of 56 mm, an outer diameter of 19 mm, and a total mass of 41 g as shown in Figure 3.

When the permanent magnet is displaced upward in Figure 1, the pressure near the valve increases. Therefore, the valve made by the thin silicon material is pushed up and liquid delivery is possible. On the other hand, when the magnet is displaced downward, the pressure near the valve decreases. Therefore, the valve closes, and backflow of fluid is prevented. Fluid is intermittently discharged by repeatedly increasing and decreasing the pressure over one cycle of vibration.

### OPTIMUM DESIGN FOR SHAPE OF THE MAGNETIC PUMP

In this paper, optimize shape for the magnetic pump was carried out for the following three items, as shown in Figure 4.

- ① Clearance between electromagnet and casing:  $C$  (mm)
- ② Thickness of the thin silicone valve:  $h$  (mm)
- ③ Diameter of hole in valve:  $d$  (mm)

Water was selected as a fluid in this experiment. The prototype pump was inserted into a water tank with a width of 350 mm, a length of 250 mm and a height of 200 mm. The a mass flow and an efficiency were measured with a pumping head of 200 mm as shown in Figure 4. The acrylic pipe having an outer diameter of 8 mm and an inner diameter of 6 mm was used as a pipe for the pumping head. The vibration component was driven at the resonance frequency using a function signal generator and an amplifier. The resonance frequency was

96 Hz. Input voltage, current and power to the electromagnet were measured using a power analyzer.

The efficiency  $\eta$  of the magnetic pump is expressed as

$$\eta = 100 M_f G (L / t) / P \quad (1)$$

Where  $M_f$  (kg) is the mass flow,  $G$  ( $m/s^2$ ) is the acceleration due to gravity,  $L$  (m) is the pumping head,  $t$  (s) is the measurement time and  $P$  (W) is the input power. The mass flow was measured with an electronic balance. The measurement time of the mass flow is 30 seconds.

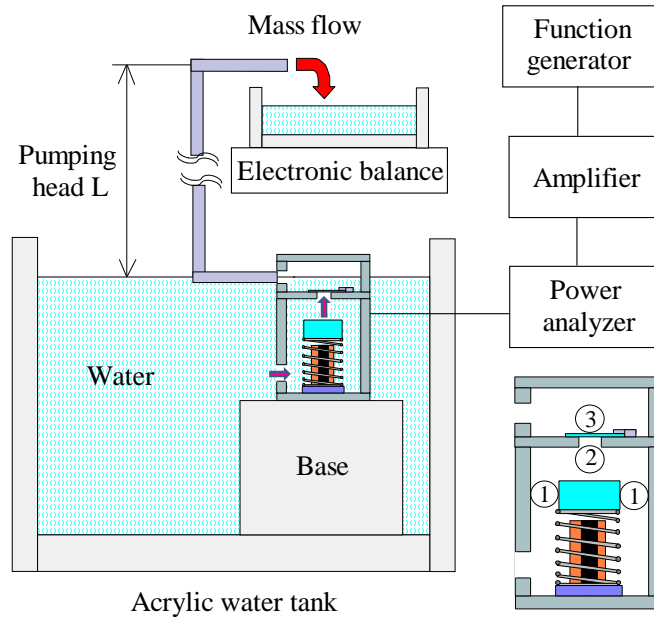


Figure 4. Experimental apparatus and optimization procedure.

Figure 5 shows the relationship between an input current to the electromagnet and the mass flow rate per unit time as the pumping head  $L = 200$  mm,  $h = 0.3$  mm and  $d = 4$  mm, when the clearance  $C$  between the permanent magnet and the casing changes to 1.5 mm, 2 mm, 3 mm and 4 mm. When the clearance becomes smaller than 1 mm, the influence of the vibration damper is generated, the displacement of the vibration component becomes very small.

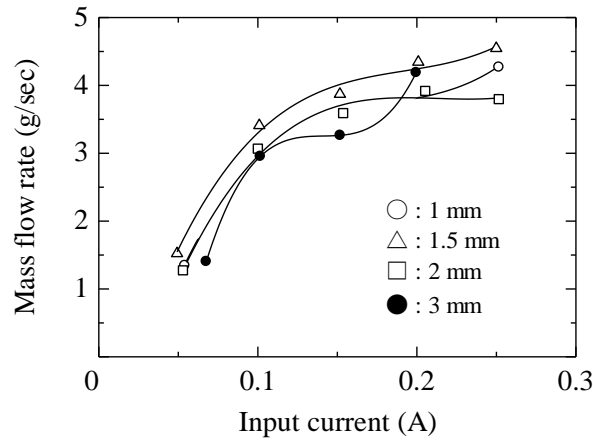


Figure 5. Relationship between input current and mass flow rate.

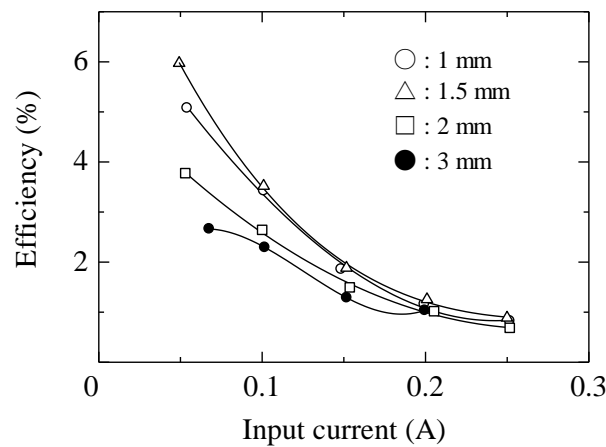


Figure 6. Relationship between input current and efficiency.

On the other hand, Figure 6 shows the relationship between the input current and the efficiency with the same clearance  $C$ , the pumping head  $L$ , valve thickness  $h$  and diameter  $d$  as shown in Figure 4. When the clearance  $C$  was 1.5 mm, the maximum efficiency of the magnetic pump demonstrates 6.0 %. From the results of Figures 5 and 6, when the clearance between the permanent magnet and the casing becomes small, the amplitude of the vibration component becomes small due to the influence of viscous damping by water. Since this pump does not have a suction valve, when the clearance between them becomes large, the pressure decreases and the flow rate characteristic decreases. When the clearance between them is 1.5 mm, above two effects are balanced and an optimum characteristic is generated.

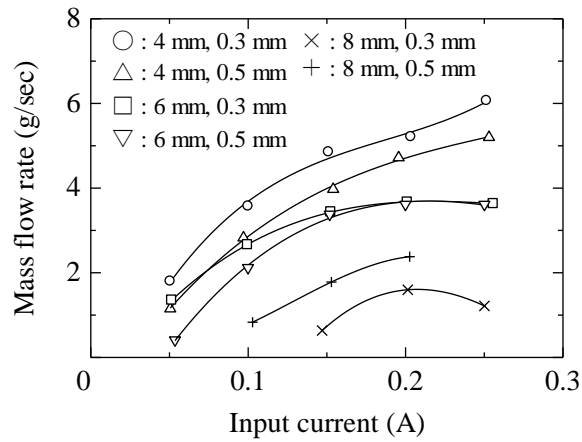


Figure 7. Relationship between input current and mass flow rate.

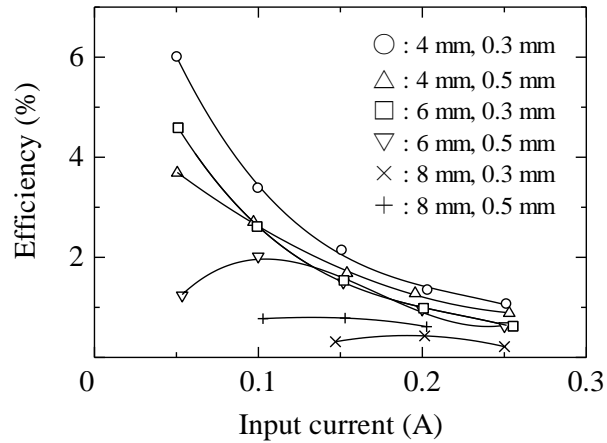


Figure 8. Relationship between input current and efficiency.

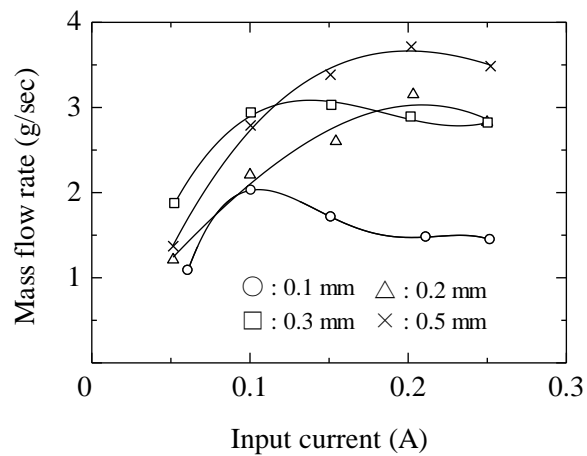


Figure 9. Relationship between input current and mass flow rate.

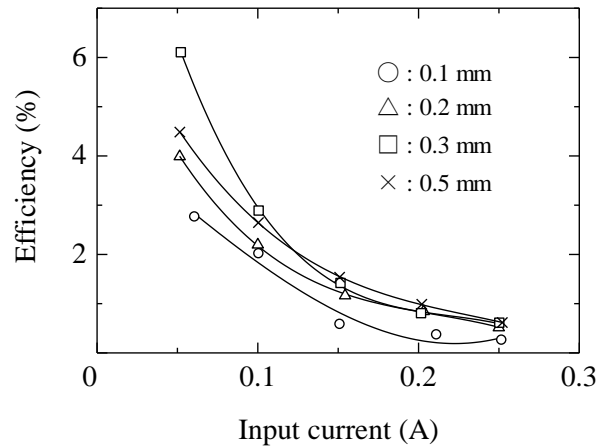


Figure 10. Relationship between input current and efficiency.

As a parameter thickness  $C$  of thin silicone valve and diameter  $d$  of hole for valve, Figure 7 shows the relationship between the input current to the electromagnet and the mass flow rate per unit time as the pumping head  $L = 200$  mm,  $C = 1.5$  mm. On the other hand, Figure 8 shows the relationship between the input current and the efficiency with the same parameter as Figure 7. When thickness  $h$  of thin silicone valve was 0.3 mm and diameter  $d$  of hole in valve was 4 mm, the magnetic pump demonstrates the maximum efficiency. As described above, since this pump has no the suction valve, it is considered that optimum values exist for the diameters of the permanent magnets and all amplitudes of the vibration component.

Finally, as a parameter thickness  $h$  of silicone valve, Figure 9 shows the relationship between the input current to the electromagnet and the mass flow rate per unit time as the pumping head  $L = 200$  mm,  $C = 1.5$  mm,  $d = 4$  mm. Figure 10 shows the relationship between the input current and the efficiency with the same parameter as Figure 9. When thickness  $h$  of silicone valve was 0.3 mm, the efficiency of the magnetic pump demonstrates the maximum value. When the thickness of the silicone rubber becomes large, a high pressure is required in the casing to exhaust water. On the other hand, when the thickness decreases, the water discharge effect disappears due to the elastic deformation of the material itself. For these reasons, the valve thickness of 0.3 mm gives an optimum value.

For the proposed magnetic pump in this paper, the shape was optimized and clearance  $C = 15$  mm,  $h = 0.3$  mm,  $d = 4$  mm was determined, respectively. Thereafter, the flow characteristics of the magnetic pump were measured using the above parameter values. In this experiment, optimization of the casing and the valve was carried out unified to the head of 200 mm. However, it is expected that optimum values will exist for each pumping head.

## FLOW CHARACTERISTICS OF PUMP WITH OPTIMIZED SHAPE

For the magnetic pump with the optimized shape, Figure 11 shows the relationship between the input current, and the mass flow rate per unit time and the efficiency when the pumping head  $L$  was 200 mm. In this figure,  $\circ$  and  $\triangle$  indicate the experimental values for the mass flow rate and efficiency, respectively. When the input current to the electromagnet was 0.05 A, the maximum efficiency of the pump was about 6.0 %.

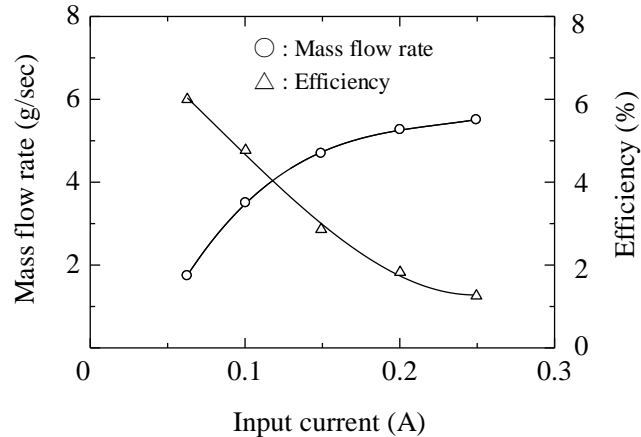


Figure 11. Relationship between input current and mass flow rate, and efficiency.

## IMPROVEMENT OF EFFICIENCY BY ATTACHING IRON PLATE

A novel magnetic pump was proposed and tested. However, the efficiency of the pump was not high. An effective method of improving efficiency is newly proposed. When a copper wire is symmetrically wound around an iron core to create the electromagnet, a magnetic field with the same strength at each magnetic pole of the iron core is formed. Conversely, when a copper wire is asymmetrically wound around the iron core, an asymmetric magnetic field is formed. The strength of the magnetic field at one pole of the electromagnet can be increased by utilizing asymmetric windings, as mentioned above.

A method of increasing the efficiency of the magnetic pump was suggested as shown in previous study [33]. Before the experiment was performed, the magnetic flux density of the electromagnet was calculated using two-dimensional finite element analysis software. In the case where the electromagnet and the permanent magnet as shown in Figure 12 are used, Figure 13 shows the flow of magnetic flux as the iron plate with a diameter of 20 mm and a thickness of 1 mm is attached to one edge of the electromagnet. When the iron plate was added to the electromagnet, the electromagnetic force between the electromagnet and the permanent magnet increased more than in the case without the iron plate. It was confirmed by numerical simulation that the magnetic flux density of the electromagnet increased when the iron plate was attached to the iron core.

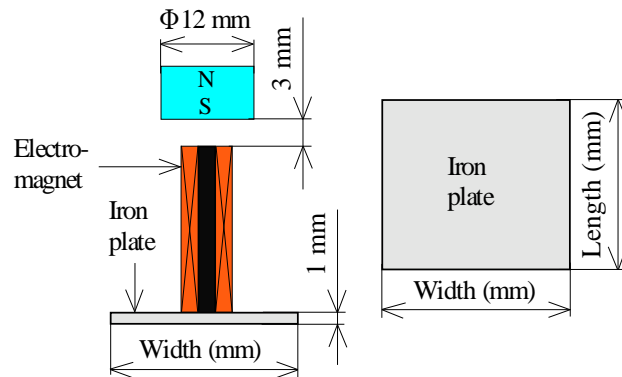


Figure 12. Electromagnet with attached iron plate.

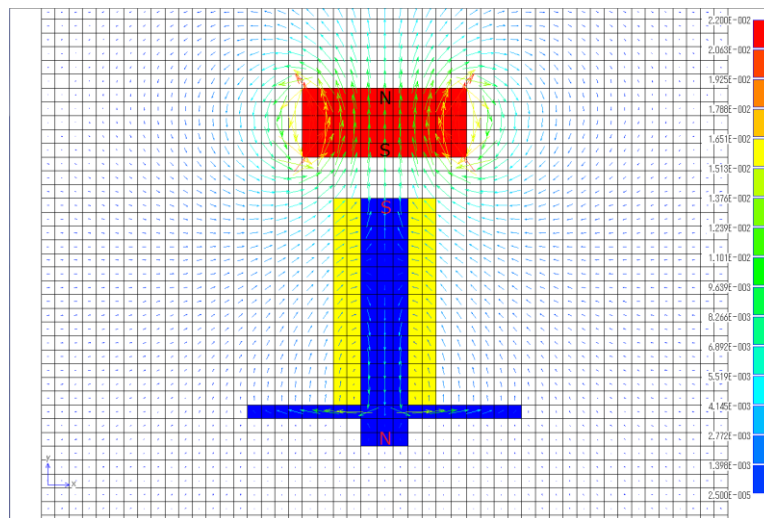


Figure 13. Magnetic flux flow.

Based on these simulation results, iron plates of three sizes were used in the experiment. Sizes of all iron plates are listed in Table 1, where Type I is the case without the iron plate and Types II, III, and IV indicate three iron plates of different sizes. The magnetic flux density of the iron core for the electromagnet with the iron plate attached to one edge was measured using the tesla meter. A direct current of 0.05 A to 0.25 A was applied to the electromagnet during the measurement. Figure 14 shows the vibration component with various iron plate, respectively.

Figure 15 shows the relationship between the input current to the electromagnet and the magnetic flux density measured for all iron plates sizes considered in experiment. The average value of the magnetic flux density increased with increasing plate size. An average of the magnetic flux density for the Type II, III, and IV iron plates were 1.15, 1.27 and 1.37 times that of Type I, respectively.

Table 1. Sizes of iron plates.

Type	Length (mm)	Width (mm)	Thickness (mm)
Type I (Acrylic)	0	0	0
Type II (Iron plate)	20	20	1
Type III (Iron plate)	30	30	1
Type IV (Iron plate)	40	40	1

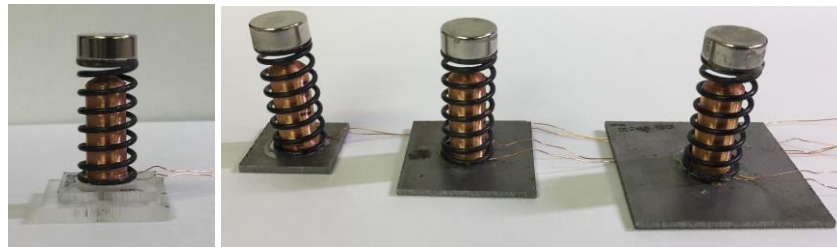


Figure 14. Photograph of each vibration component.

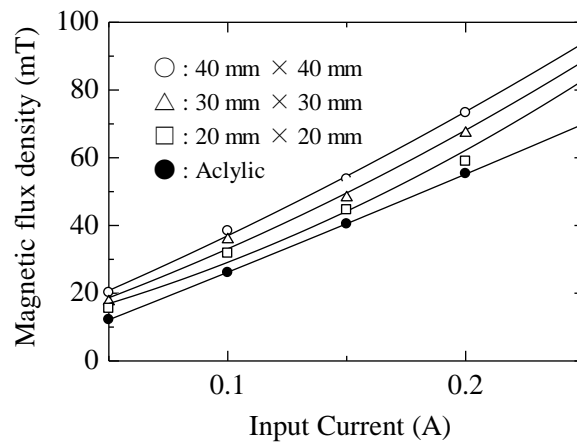


Figure 15. Relationship between input current and magnetic flux density.

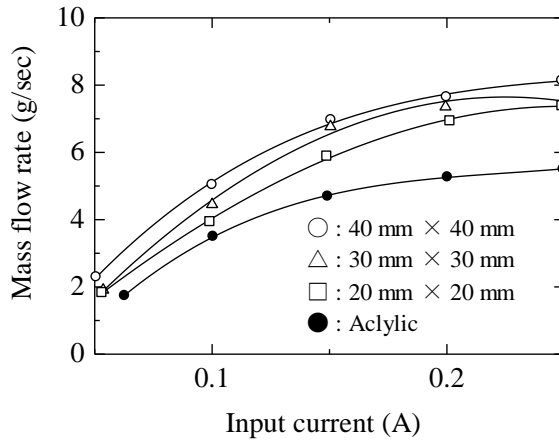


Figure 16. Relationship between input current and efficiency.

Figure 16 shows the relationship between the input current and the mass flow rate per unit time for all iron plate sizes considered in experiment. On the other hand, Figure 17 shows the relationship between the input current and the efficiency. By adding the iron plate with a width of 40 mm and a length of 40 mm, the maximum efficiency of the magnetic pump increased to 10.7 %.

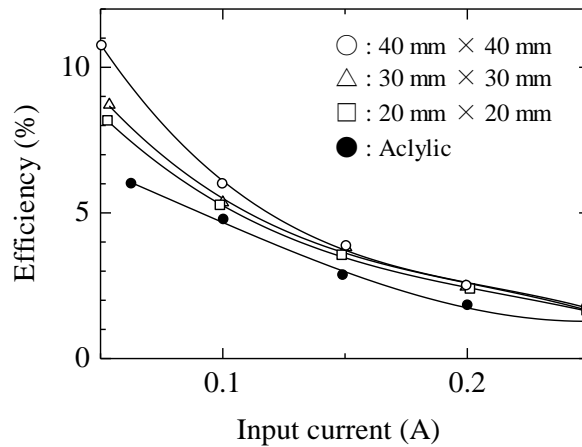


Figure 17. Relationship between input current and efficiency.

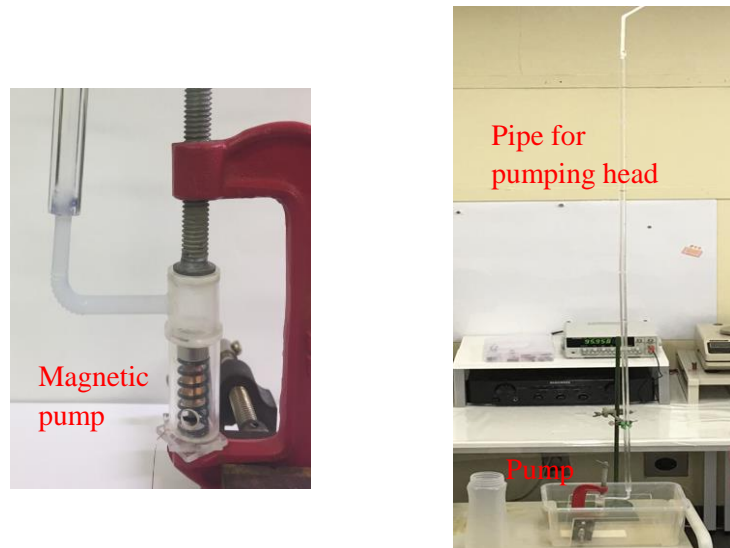


Figure 18. Magnetic pump with pumping head of 1000 mm.

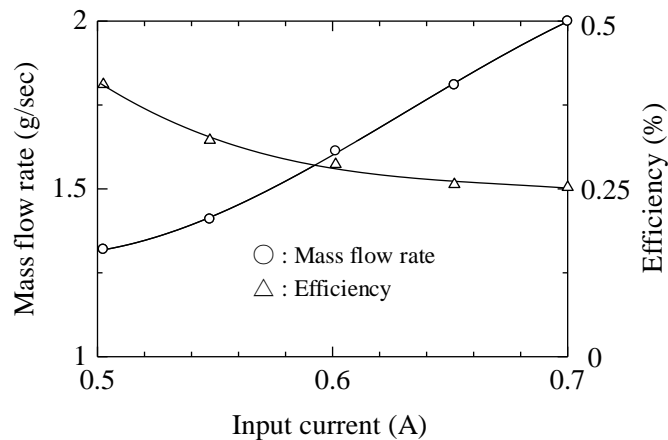


Figure 19. Relationship between input current and mass flow rate, and efficiency.

Therefore, the Type III iron plate was used in the next experiment. The flow rate characteristics of the magnetic pump were measured when the pumping head  $L$  was extended to 1000 mm. The outline of the pump is shown in the photograph of Figure 18.

In summary, by asymmetric magnetic field due to addition of the iron plate, the increase in the magnetic flux density increases the electromagnetic force. In addition, as the electromagnetic force increases, the displacement amplitude of the vibration component linearly increases. A linear increase in the displacement amplitude increases the kinetic energy (elastic energy) quadratically, so that a great improvement in the flow efficiency can be obtained. As described in the introduction, a lot of new principle pumps have been proposed [1-14]. Although it is larger in size than these pumps, only this magnetic pump seems to indicate efficiency exceeding 10 %.

## CONCLUSION

A novel magnetic pump combining electromagnetic force and mechanical vibration has been proposed and the optimum design of the pump shape was carried out. The magnetic pump with optimized shape demonstrated a maximum efficiency of 6.0 %.

On the other hand, based on the fact that an asymmetric electromagnet produces an asymmetric magnetic field, a method of increasing the magnetic field strength at one pole of the electromagnet by attaching an iron plate was proposed. By the generation of an asymmetric magnetic field due to the addition of the iron material, the maximum efficiency of the pump was 10.7 %. In addition, this small size pump has a very simple structure and can deliver water to the pumping head exceeding 1000 mm.

## REFERENCES

- [1] Momosaki S, Usami S, Watanabe S, Furukawa A, Okuma K. Experimental Study on Rotational Speed Control of Contra-Rotating Axial Flow Pump. *Journal of TSJ*. 2011;39:119-25.
- [2] Yasuyuki N, Junichiro F. Effect of Impeller Outlet Width on Radial Thrust of Single-Blade Centrifugal Pump with a Helical Spiral Suction Flow Channel. *Journal of TSJ*. 2011;39:47-56.
- [3] Benra FK. Experimental Investigation of Hydrodynamic Forces for Different Configurations of Single-Blade Centrifugal Pumps. *The 11 International Symposium on Transport Phenomena and Dynamics of Rotating Machinery (ISROMAC-11)*. 2011;2011:24-30.
- [4] Shigemitsu T, Fukutomi J, Takumi M, Masahiro S. Unsteady Flow Condition of Centrifugal Pump for Low Viscous Fluid Food. *International Journal of Fluid Machinery and Systems*. 2017;10:432-38.
- [5] Nishi Y, Fukutomi J, Shigemitsu T, Higashide S. Improvement of Instability Characteristics in a Mixed-Flow Pump Based on Flow near Blade Tip. *The Japan Society of Mechanical Engineers*. 2011;77:1484-92.
- [6] Day IJ. Active Suppression of Rotating Stall and Surge in Axial Compressors. *ASME Journal of Turbomachinery*. 1993;115:40-7.
- [7] Houzeaux G, Codina R. A finite element method for the solution of rotary pumps. *Comput. Fluids*. 2007;36:667-79.
- [8] Voorde JV, Vierendeels J, Dick E. Flow simulations in rotary volumetric pumps and compressors with the fictitious domain method. *Comput. Method Appl. Math*. 2004;168:491-9.
- [9] Kang YH, Vu HH. A newly developed rotor profile for lobe pumps. *Journal of Mechanical Science and Technology*. 2014;28:915-26.
- [10] Kang YH, Vu HH, Hsu CH. Factors impacting on performance of lobe pumps. A numerical evaluation (*J. Mech*). 2012;28:229-38.
- [11] Houzeaux G, Codina R. A finite element method for the solution of rotary pumps. *Comput. Fluids*. 2007;36:667-79.

- [12] Voorde JV, Vierendeels J, Dick E. Flow simulations in rotary volumetric pumps and compressors with the fictitious domain method. *Comput. Method Appl. Math.* 2004;168:491-9.
- [13] Kurita H. Pump design for the next generation. *Journal of the JIME.* 2015;50:97-100.
- [14] Ohshima M. Efficiency Increase and Input Power Decrease of Converted Prototype Pump Performance. *Turbomachinery Society of Japan.* 2011;39:712-21.
- [15] Yin H, Huang H, Fang Y, Hsieh W. A novel electromagnetic elastomer membrane actuator with a semi-embedded coil. *Sensor and Actuator.* 2007;139:194-202.
- [16] Lee GH, Kim HR. Design analysis of DC electromagnetic pump for liquid sodium CO<sub>2</sub> reaction experimental characterization. *Annals of Nuclear Energy.* 2017;109:490-7.
- [17] Guo S, Wang J, Guo J. A Novel Type of Micropump Using Solenoid Actuator for Biomedical Applications. 2007 IEEE International Conference on Robotics and Automation. 2007;2007:654-9.
- [18] Ebrahim M. Design and simulation of a novel electrostatic peristaltic micromachined pump for drug delivery applications. *Sensor and Actuator.* 2005;117:222-9.
- [19] Kim J, Kang C, Kim Y. A disposable polydimethylsiloxane-based diffuser micropump actuated by piezoelectric-disc. *Microelectron Eng.* 2004;71:119-124.
- [20] Nguyen N, White RM. Design and optimization of an ultrasonic flexural plate wave micropump using numerical simulation. *Sensor and Actuator.* 1999;77:229-36.
- [21] Sateesh1 J, Rao K, Sravani1 K, Guha K, Kumar R. Design and Optimization of MEMS Based Piezo-ElectroMicro Pump. 4th International Conference on Microelectronics. 2017;2017:1200-6.
- [22] Leng X, Zhang J, Zhao C. A spiral-tube-type valveless piezoelectric pump with gyroscopic effect. *Chinese Science Bulletin.* 2014;59:1885-9.
- [23] Claeysen F, Lhermet N. Actuators Based on Giant Magnetostrictive Materials. 8th International Conference on New Actuators. 2002;2002:10-2.
- [24] Lu Q, Nie Q. Research on New Type of Giant Magnetostrictive PrecisionFlow Pump. International Symposium on Material. Energy and Environment Engineering. 2005;2005:DOI: 10.2991/ism3e-15.
- [25] Zhu Z, Liu F, Tao Z. A Novel Magnetostrictive Piston Pump and Its Working Performance. IEEE International Conference on Applied System Innovation. 2018;2018:DOI: 10.1109/ICASI.2018.8394341.
- [26] Quan L, Zhao Y, Nie Q. Design and Experiment of Rare Earth Giant Magnetostrictive Piston Pump. *Materials Science Forum.* 2016;852:943-51.
- [27] Kim SH, Hashi S, Ishiyama K. A Method for Acquiring the Torque of a Magnetic Pump. *IEEE Transaction on magnetics.* 2011;47:3971-4.
- [28] Kim SH, Yu CH, Ishiyama K. Tiny magnetic wireless pump: Fabrication of magnetic impeller and magnetic wireless manipulation for blood circulation in legs. *Journal of Applied Physics.* 2015;117:https://doi.org/10.1063/1.4916026.
- [29] Song MK, Kim SH. Wireless Magnetic Pump, Characteristics of Magnetic Impellers and Medical Application. *Journal of Magnetism.* 2017;22:344-51.
- [30] Guo S, Asaka K. Polymer-based New Type of Micropump for Bio-medical Application. Proceedings of 2003 IEEE International Conf. on Robotics and Automation. 2003;2003:987-92.

- [31] Sagar SN, Sreekumar M. Miniaturized Flexible Flow Pump using SMA Actuator. *Procedia Engineering*. 2013;64:896-906.
- [32] Homsy A, Linder V, Lucklum F, Rooij NF. Magneto hydrodynamic pumping in nuclear magnetic resonance environments. *Sensor and Actuator*. 2007;123:636-46.
- [33] Yaguch H, Sakuma S. Vibration Actuator Capable of Movement on Magnetic Substance Based on New Motion Principle. *Journal of Vibroengineering*. 2017;19:1494-1508.